

1 Using Electronic Theory To Identify Metabolites Present in 2 17 α -Ethinylestradiol Biotransformation Pathways

3 William J. Barr,[†] Taewoo Yi,[§] Diana Aga,[‡] Orlando Acevedo,^{||} and Willie F. Harper, Jr.*[†]

4 [†]Department of Civil and Environmental Engineering, Swanson School of Engineering, University of Pittsburgh, Pittsburgh,
5 Pennsylvania 15261, United States

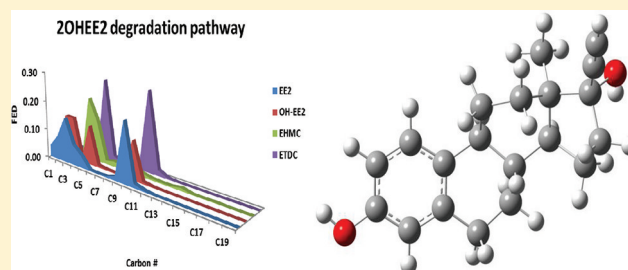
6 [§]Department of Environmental Science and Engineering, Ewha Womans University, Seoul, 120-750 Korea

7 [‡]Department of Chemistry, University at Buffalo, The State University of New York, Buffalo, New York 14260, United States

8 ^{||}Department of Chemistry and Biochemistry, Auburn University, Auburn, Alabama 36849, United States

9 **S** Supporting Information

10 **ABSTRACT:** This research used electronic theory to model
11 the biotransformation of 17 α -ethinylestradiol (EE₂) under
12 aerobic conditions in mixed culture. The methodology involved
13 determining the Frontier Electron Density (FED) for EE₂ and
14 various metabolites, as well as invoking well-established degra-
15 dation rules to predict transformation pathways. We show that
16 measured EE₂ metabolites are in good agreement with what
17 is expected based on FED-based modeling. Initiating reactions
18 occur at Ring A, producing metabolites that have been experi-
19 mentally detected. When OH-EE₂ and 6AH-EE₂ are trans-
20 formed, Ring A is cleaved before Ring B. The metabolites involved in these pathways have different estrogenic potentials, as
21 implied by our analysis of the log P values and the hydrogen bonding characteristics. The OH-EE₂ and 6AH-EE₂ transformation
22 pathways also show redox-induced electron rearrangement (RIER), where oxidation reactions lead to the reduction of carbon
23 units present along the bond axis. Sulfo-EE₂ appears to be difficult to biotransform. These findings clarify theoretical and practical
24 aspects of EE₂ biotransformation.



25 ■ INTRODUCTION

26 The presence of 17 α -ethinylestradiol (EE₂) in the aquatic
27 environment continues to be a topic of considerable interest to
28 the water quality community. It is an anthropogenic pollutant
29 that is present in rivers, lakes, and groundwaters,^{1–3} and it
30 induces developmental anomalies in wildlife (such as feminized
31 male fish).^{4–7} Negative ecological impacts may occur at very low
32 concentrations (i.e., ppb or ppt). EE₂ is primarily introduced
33 into the aquatic environment via domestic wastewater, so sew-
34 age treatment processes are critical for eliminating EE₂ from
35 the water cycle. Learning more about the removal of EE₂ is an
36 important priority; we need to discover the transformation
37 pathways, and we also need to learn how to minimize or
38 remove the toxicity of the resulting byproducts.

39 It is now clear that EE₂ can be removed during the activated
40 sludge process. Numerous studies have biologically degraded
41 EE₂ under aerobic conditions,^{8–10} and a number of studies have
42 carried out these studies in the concentration range (i.e., low
43 $\mu\text{g/L}$ or ng/L) expected in real wastewater.^{11,12} Some studies
44 have detected metabolites using tools like NMR⁸ or LC/MS/
45 MS,¹³ but most of the previous research has reported EE₂
46 removal without reconciling its ultimate fate or identifying
47 byproducts. Recent work has shown that EE₂ is partially miner-
48 alized (i.e., converted to carbon dioxide) during aerobic treat-
49 ment of sewage. For example Yi et al., 2011¹⁴ degraded EE₂ in

fed-batch bioreactors and measured 40–60% conversion to 50
carbon dioxide. Khunjar et al., 2011¹³ degraded EE₂ in aerobic 51
chemostats, and they measured 13% and 26% EE₂ conversion 52
to carbon dioxide. Both of these reports show that it is possible 53
to mineralize EE₂ and its byproducts from water, but, in each 54
case, a significant fraction of ¹⁴C-EE₂ remained in the waste- 55
water either in the aqueous phase or associated with suspended 56
solids. EE₂ can be removed during the activated sludge process, 57
but there are lingering concerns related to the byproducts. This 58
is, therefore, an appropriate moment to discover important 59
components of the biotransformation pathways. 60

Ring cleavage is a key event in the EE₂ transformation 61
pathway because, without rings, the metabolites are easier to 62
assimilate¹⁵ and unlikely to bind to estrogen receptors.¹⁶ 63
Understanding EE₂ ring cleavage would allow us to better 64
understand the intermediates that may be present in wastewater 65
effluents (including those that are difficult to detect analyti- 66
cally). The current metabolite data set has also lead to some 67
apparently conflicting ideas about EE₂ ring cleavage. For 68
example, Yi and Harper, 2007⁸ and Khunjar et al., 2011¹³ both 69

Received: May 24, 2011

Revised: November 22, 2011

Accepted: November 30, 2011

70 reported metabolites that show that ring A is the first to be
71 cleaved during biotransformation. Their results are in conflict
72 with those of Haiyan et al., 2007,¹⁷ who used *Sphingobacter-*
73 *ium* sp. JCRS to degrade EE₂, and, based on the daughter
74 products they detected, they proposed that EE₂ is initially
75 oxidized to estrone, followed by ring B (not ring A) cleavage.
76 Collecting more metabolite data and modeling biotransfor-
77 mation reactions can address and resolve questions related to
78 ring cleavage.

79 Identifying byproducts will also address concerns related
80 to estrogenicity, which in turn, is influenced by chemical struc-
81 tures. For example, Fang et al., 2001¹⁶ analyzed 230 natural and
82 synthetic steroids (with and without phenolic rings), and they
83 found that the number of hydrogen bond donating groups (n_d)
84 correlated negatively with estrogenicity. They also found that
85 the octanol–water partitioning coefficient ($\log P$) was posi-
86 tively correlated with estrogenicity, because compounds with
87 relatively low $\log P$ values were more soluble and less likely to
88 interact with hormone receptors. Lipinski et al., 2001¹⁸ found
89 similar results for their analysis of approximately 2500 organic
90 compounds. Schultz et al., 2001¹⁹ developed structure–activity
91 relationships for 120 aromatic compounds, and they found
92 that n_d correlated well with estrogenicity. They found that the
93 number of hydrogen bond accepting groups (n_a) was negatively
94 correlated with estrogenicity. They also found that the hydro-
95 phobicity of rings B, C, and D (but not A) was positively
96 correlated with estrogenicity. These parameters ($\log P$, n_d , n_a)
97 can be determined from the chemical structures of EE₂ and
98 its metabolites. Therefore, it is possible to assess the estrogenic
99 potential associated with compounds involved in biotransfor-
100 mation pathways.

101 The current work aims to apply frontier electron density
102 (FED) theory to explore EE₂ biotransformation. FED calcula-
103 tions can elucidate the fundamental principles governing EE₂
104 reactivity by predicting which positions on the molecule will
105 most likely undergo electrophilic attack. Of particular impor-
106 tance is the localization of the highest occupied molecular orbital
107 (HOMO), as electrons occupying this frontier orbital are most
108 free to participate in the initiating reactions. The general con-
109 cept is that an electron-poor molecule will readily attack a posi-
110 tion of large electron density. Fukui developed the powerful
111 FED model for describing chemical reactivity via frontier mole-
112 cular orbital (FMO) theory and pioneered much of the early
113 work connecting FED to chemical reactivity in aromatic hydro-
114 carbons.²⁰ Wheland and Pauling, 1935²¹ successfully used FED
115 to explain the reactivity of substituted aromatics. More recently,
116 Ohko et al., 2002²² using FED to explain the initiating reactions
117 associated with the photocatalysis of 17 β -estradiol, and Ohura
118 et al., 2005²³ showed that air-borne polycyclic aromatic hydro-
119 carbons were abiotically chlorinated in positions that corre-
120 sponded to high FED. Lee et al., 2001²⁴ used Fenton oxidation
121 to remove polycyclic aromatic hydrocarbons, and they success-
122 fully used FED to predict the order of daughter product pro-
123 duction. Although these previous attempts focused on
124 abiotic reactions, they bolster the potential for predicting
125 biological oxidations in the same way. Prior efforts to
126 conduct *a priori* predictions of biodegradation have been very
127 successful when focusing on readily degradable substrates
128 (e.g., glucose) that enter well-characterized metabolic
129 pathways (e.g., glycolysis). FED-based techniques present
130 the promise of predicting biodegradation on complex
131 organics like EE₂; a contribution here can eventually make
132 a significant impact. The specific objective of this work is to

compare measured EE₂ metabolites to those predicted by FED-
based theory. We intended to gain theoretical and practical
insights into EE₂ biotransformation steps as well as the nature
of the metabolites that are generated.

■ EXPERIMENTAL SECTION

Overall Approach. We simulated the transformation of
EE₂ using FED-based modeling, which consisted of
calculating the FED of all of the carbon units and then
simulating transformation according to degradation rules.
These simulations assume that a wide range of nonspecific
enzymes (e.g., oxygenases) are active. We then compared the
computational results to the identity of the measured
metabolites reported in literature (including those reported
from our lab). We also analyzed the results of ¹⁴C-EE₂
experiments done in Dr. Willie Harper's lab and used these
chromatograms to propose additional metabolites (including
a few that had not been previously reported). We used the
chemical structures to evaluate estrogenic potential; this is
related to (but not the same as) estrogenicity, which also
depends on the regulation of complex endocrine pathways.²⁵
Finally, we restricted the scope of this work to include
EE₂ transformation steps leading up to (or immediately
following) the first ring cleavage. This limitation confined
the study to the range where the majority of measured
metabolites are located.

¹⁴C-EE₂ Experiments and Metabolite Identification.
These studies were conducted with ¹⁴C-labeled ethinylestradiol
(¹⁴C-EE₂) (99% pure; American Radiolabeled Chemicals, St.
Louis, MO) at room temperature. Biomass was retrieved from
parent bioreactors and used to seed two 500 mL fed-batch bio-
reactors (FBBRs) (i.e., the bioreactors were fed continuously
with substrate, but reactor volume was discharged only during
sampling periods). At the beginning of the experiment, the
FBBRs were each spiked with ¹⁴C-EE₂ at an initial concen-
tration of 24.5 μ g/L. Aqueous samples were retrieved at three
time points (1 h, 24 h, 48 h) and then subsequently delivered
to Dr. Diana Aga's laboratory for metabolite identification. The
performance of these FBBRs has been discussed previously.¹⁴
The water samples retrieved from the ¹⁴C experiments were
analyzed by liquid chromatography/mass spectrometry (LC/MS)
and LC/radiochromatographic detection as described previ-
ously.¹⁴ Since all samples contained ¹⁴C-labeled EE₂, the
analysis was performed using an Agilent 1100 HPLC equipped
with an online radiochromatographic detector (IN/US Systems,
Inc., Tampa, FL) as described previously.²⁶ After determining
the retention times of the radioactive peaks, we reinjected an
aliquot of sample into the LC column with the eluate being
split between the radioactive detector and a triple quadrupole
mass spectrometer (Agilent 6410 MSD); the splitter was put
in place to ensure that the LC/MS data corresponded with
the radioactive peaks. We used LC/MS in conjunction with a
radioactive detector to determine the m/z ratios, which were
the basis for proposed metabolite structures.

FED Analysis. Frontier electron density (FED) analyses
were performed to determine the electron density profile for
EE₂ and for relevant metabolites. The Unrestricted Hartree–
Fock (UHF) method and STO-3G basis set were employed for
initial structure optimizations using the program Gaussian 03.²⁷
UHF/6-31G(d) calculations were used for final geometry
optimizations, computing vibrational frequencies, and in
calculating the electron density of each compound. The FED
for all carbon atoms were computed using the following

195 equation

$$f_r = [2^* \sum_i (\text{Cri HOMO})^2] \quad (1)$$

196 For an electrophilic reaction, the highest occupied molecular
197 orbital (HOMO) densities are normalized by the energy of
198 the frontier molecular orbitals at ground state. The coefficient
199 of each atomic orbital, Cri, is used to produce the frontier
200 movement, where r is the number of carbon atoms in i: 2s, 2px,
201 2py, and 2pz orbitals.²⁴ In general, the highest f_r value indicates
202 the most reactive position. We also determined geometries,
203 energies, and FEDs of carbon atoms for all compounds using
204 density functional theory (DFT) at the B3LYP/6-31G(d)
205 theory level^{28,29} for comparison. All simulations were performed
206 on computers located at the Pittsburgh Supercomputer Center.
207 FED values for EE₂-related carbons were typically between 0
208 and 0.3.

209 **Degradation Rules.** FED values were used to determine
210 the location of the most reactive part in the model compounds.
211 To determine what happens at the reactive position, we invoke
212 six *degradation rules* relevant for biologically mediated electro-
213 philic reactions:^{30–39}

214 *Rule 1* – The enzyme attacks the carbon atom at the
215 highest FED. The carbon atom being oxidized must be
216 bound to a –H, =O, or –OH group.

217 *Rule 2* – The phenol ring is cleaved after being oxidized
218 to catechol. Oxygenolytic cleavage of the phenol ring
219 occurs via *ortho*- or *meta*-cleavage. Ring cleavage takes
220 place between the hydroxylated carbon with highest FED
221 value and carbon with higher FED out of two adjacent
222 carbons.

223 *Rule 3* – The cyclohexane and cyclopentane rings are
224 opened after oxidation to cyclohexanone and cyclopenta-
225 none, respectively. Ring cleavage of either cyclohexanone
226 or cyclopentanone is determined by the same rule with
227 phenol ring cleavage.

228 *Rule 4* – After ring cleavage, carbon chains are degraded
229 to hydroxyl-, ketone, and carboxylic acid, followed by a
230 decarboxylation step.

231 *Rule 5* – Resonance can cause the phenol ring to be con-
232 verted to a semiquinone tautomer, which can be oxidized
233 according to degradation rules 1–4.

234 *Rule 6* – If the degradation rules are not applicable
235 to rules 1 through 4, enzymatic attack proceeds at the
236 carbon atom with the second highest FED value.

237 **Estrogenicity.** We examined estrogenic characteristics by
238 calculating the log P and the number of hydrogen bond donors
239 and acceptors. We calculated both of these parameters using
240 the atom-based additive approach.⁴⁰

241 ■ RESULTS

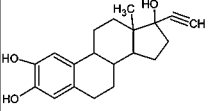
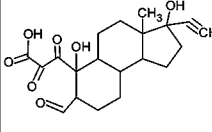
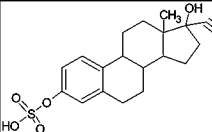
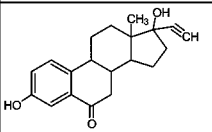
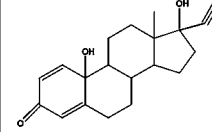
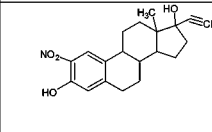
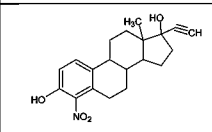
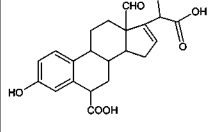
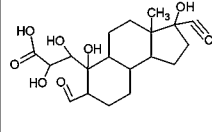
242 Proposed structures for the metabolites detected from the ¹⁴C
243 experiments are shown in Table 1. Two of the quickly pro-
244 duced (i.e., after 1 h of reaction time) metabolites are M312
245 and M376 (corresponding to m/z 311 and m/z 375 peaks in
246 negative ESI MS), and their proposed identities are OH-EE₂
247 and SO₄-EE₂ (Sulfo-EE₂) respectively. These structures suggest
248 hydroxyl- and sulfo-transfer initiating reactions that can be
249 carried out by a wide range of common oxygenase and sulfo-
250 transferase enzyme.^{15,41} The identities of these initial meta-
251 bolites are supported by Yi and Harper, 2007,⁸ who detected
252 both of them from a nitrifying membrane bioreactor using thin

layer chromatography and NMR. The metabolite M310
(m/z 309) is EDMO, a byproduct that shows the presence of a
(m/z 309) is EDMO, a byproduct that shows the presence of a
ketone group on ring B. M385 is DOEF, which shows that
the ethinyl group has been converted to a carboxylate group,
and that a carboxylation reaction takes place at ring B. The
proposed structure for M314 (m/z 313) is 6AH-EE₂; this
metabolite has been measured by Della-Greca et al., 2008,⁴² and
its formation is not surprising because the C10 carbon unit has
high frontier electron density (C10 = 0.38) and it is therefore
an attractive location for electrophilic modification. Finally,
M341 (m/z 340) is either 2 Nitro-EE₂ or 4 Nitro-EE₂; both
formed by way of an abiotic nitration reaction.¹¹ This collection
of metabolites is largely consistent with what has been detected
previously from nitrifying mixed cultures.^{8,13,26}

We now turn our attention to FED-based prediction of EE₂
metabolism. Figure 1 shows EE₂ and three initial metabolites.
The chemical convention used here denotes rings A through D
as shown in the parent structure in the upper left-hand corner
of Figure 1. Ring A of EE₂ contains several high FED C units
(1–5 and 10), making it the most attractive location for elec-
trophilic modification. The reactions reflected by the structure
of these initial metabolites are consistent with ring A modi-
fications. OH-EE₂, detected in the current study and in two
previous reports, is hydroxylated at carbon unit 2 (C₂ FED =
0.1), while both Sulfo-EE₂ and EHMD are modified at C3
(FED = 0.16). These initiating reactions support the idea of
using FED theory to explore biologically mediated initiating
reactions, and we also extract two additional points from Figure 1.
First, EE₂ C10 has the highest FED value, but initial hydro-
xylations are unlikely to occur at this site because C10 is not
bound to an –OH, =O, or –H group (see Rule 1). Second, the
two levels of theory both point to the same carbon units as
likely reaction sites. This is an important insight. UHF theory is
among the most common methods for determining FED. The
disadvantage of this method is that it uses a crude central field
approximation to account for electron–electron interactions,
rendering it more inaccurate. Density functional theory accounts
for electron–electron interactions more rigorously. Our results
show that UHF can provide useful information related to EE₂
initiating reactions.

The initial metabolites can be further degraded to other
byproducts. Figure 2 shows a metabolic pathway from EE₂ to
ETDC. Ring A cleavage occurs between C2 and C3 because
of oxygenolytic activity typically carried out by dioxygenases,⁴³
and this ring cleavage step causes a dramatic extraction of
electrons, decreasing the FED of C2 (0.15 to 0.005), C3 (0.14
to >0.001), and C10 (0.13 to 0.013). There is also an interest-
ing increase in the FED of C4 (<0.001 to 0.1), consistent with
the idea that removing electrons can cause the electron density
along the C–C bond to increase. This is computationally possi-
ble because the nucleophilic Fukui function (the mathematical
underpinning of FED-based calculations) can take on negative
values (in contrast to the basis of tradition, simple frontier
molecular orbital theory). The nucleophilic Fukui function is a
key indicator of redox-induced electron rearrangement (RIER),
where oxidation of a particular molecule can lead to the reduc-
tion of a specific region of the molecule (usually along the bond
axis, between the carbon atoms). Melin et al., 2007⁴⁴ docu-
mented similar observations while studying the oxidation of
substituted acetylenes. Overall, these results make three im-
portant points. First, they show an example of a synthetically
generated degradation pathway that predicted two measured
metabolites (OH-EE₂, ETDC). Second, they demonstrate that

Table 1. Metabolites Identified in Current Study

m/z	Proposed structure	IUPAC name	Abbreviation	Analytical conformation	Reported by others
311		17-ethynyl-13-methyl-7,8,9,11,12,14,15,16-octahydro-6H-cyclopenta[a]phenanthrene-2,3,17-triol	OH-EE ₂	dansyl chloride derivatization - Positive	Yi and Harper, 2007; Skotnicka-Pitak <i>et. al.</i> , 2009
375		3-(3-ethynyl-7-formyl-3,6-dihydroxy-3a-methyl-1,2,4,5,5a,7,8,9,9a,9b-decahydrocyclopenta[a]naphthalen-6-yl)-2,3-dioxo-propanoic acid	O-DNDPA	dansyl chloride derivatization - Negative	NO
		(17-ethynyl-17-hydroxy-13-methyl-7,8,9,11,12,14,15,16-octahydro-6H-cyclopenta[a]phenanthren-3-yl) hydrogen sulfate	Sulfate-EE ₂	NO	Yi and Harper, 2007
309		17-ethynyl-3,17-dihydroxy-13-methyl-7,8,9,11,12,14,15,16-octahydrocyclopenta[a]phenanthren-6-one	OPO	dansyl chloride derivatization - Positive	NO
313		17-ethynyl-10,17-dihydroxy-13-methyl-6,7,8,9,10,11,12,13,14,15,16,17-dodecahydro-3H-cyclopenta[a]phenanthren-3-one	6AH-EE ₂	No	Della-Greca <i>et. al.</i> 2008
340		17-ethynyl-13-methyl-2-nitro-7,8,9,11,12,14,15,16-octahydro-6H-cyclopenta[a]phenanthrene-3,17-diol	2 Nitro-EE ₂	dansyl chloride derivatization - Positive	Skotnicka-Pitak <i>et. al.</i> , 2009; Gaulke <i>et. al.</i> , 2008
		17-ethynyl-13-methyl-4-nitro-7,8,9,11,12,14,15,16-octahydro-6H-cyclopenta[a]phenanthrene-3,17-diol	4 Nitro-EE ₂	dansyl chloride derivatization - Positive	Skotnicka-Pitak <i>et. al.</i> , 2009; Gaulke <i>et. al.</i> , 2008
385		17-(1,2-dihydroxy-2-oxo-ethyl)-13-formyl-3-hydroxy-6,7,8,9,11,12,14,15-octahydrocyclopenta[a]phenanthrene-6-carboxylic acid	OPCA	dansyl chloride derivatization - Positive	Skotnicka-Pitak <i>et. al.</i> , 2009
379		3-(3-ethynyl-7-formyl-3,6-dihydroxy-3a-methyl-1,2,4,5,5a,7,8,9,9a,9b-decahydrocyclopenta[a]naphthalen-6-yl)-2,3-dihydroxy-propanoic acid	DNDPA	dansyl chloride derivatization - Positive	NO
293	Unknown	Unknown	Unk.	dansyl chloride derivatization - Positive	NO

ring A is cleaved before ring B, and third, these results support RIER, which allows the Fukui function to be negative and the FED of nearby carbon units to increase during oxidation reactions.

Figure 1S also shows the metabolic pathway from EE₂ to EDMC via 6AH-EE₂. The first step is a tautomerization at C3

(FED = 0.153), which has one of the highest FED values on the parent compound. The second step is a hydroxylation at C10 resulting in a metabolite (6AH-EE₂) that was generated by an enriched Sphingomonas culture.⁴² During this step, the FED decreased in each carbon unit, except for C5, which more than doubled (0.018 to 0.037). Ring A is cleaved between C2 and

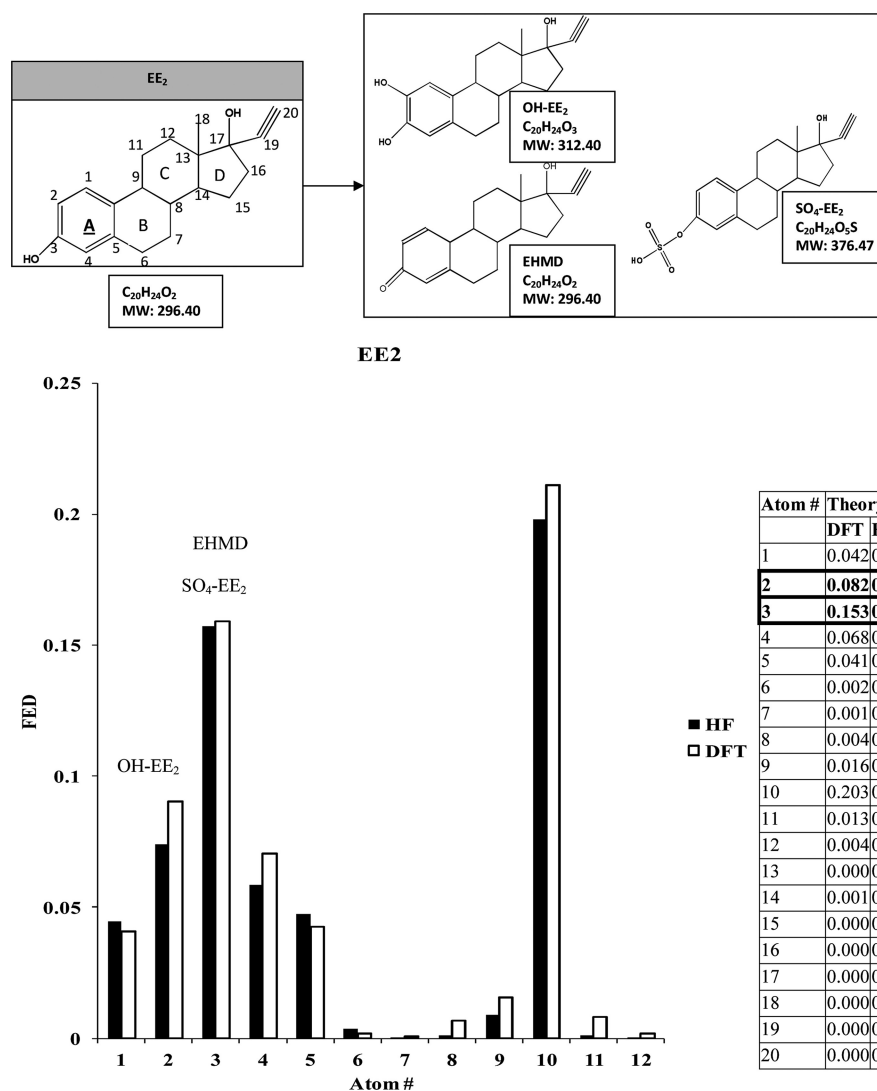


Figure 1. FED profile for EE₂. Three initial metabolites are shown at the corresponding reaction sites.

328 C3 after oxidation at C2, and then the degradation of the
 329 carboxylic groups in CEDM accounts for the production of the
 330 last metabolite shown in this pathway. This pathway supports
 331 the notation that ring A is cleaved before ring B, and it provides
 332 another example of RIER.

333 The third initial metabolite of interest in this study is Sulfo-
 334 EE₂ (Figure 2S). This metabolite has been identified in the
 335 current study and in two previous studies that transformed EE₂
 336 using mixed cultures of activated sludge. The FED profile of
 337 Sulfo-EE₂ shows that the highest FED value resides at C10 (0.2).
 338 Hydroxylation of C10 is possible in principle, but the ensuing
 339 transformation at ring A cannot be theoretically predicted at
 340 this time because there are no established biological degrada-
 341 tion rules that account for the presence of the sulfate group at
 342 C3. Further, redox reactions involving the sulfur unit are pre-
 343 cluded from the current approach because of its low FED value
 344 (<0.01). In situ, there are sulfotransferase and sulfatase enzymes
 345 that can, in principle, transform Sulfo-EE₂ (or related structures).
 346 However, these activities are not predicted using FED-based
 347 theory. It is also interesting to note that Sulfo-EE₂ appears to
 348 be more recalcitrant than OH-EE₂ or 6AH-EE₂. Khunjar et al.,
 349 2011¹³ recently found that Sulfo-EE₂ produced by a nitrifying
 350 culture was not degraded further by a heterotrophic culture that

was placed in series. Their findings imply that Sulfo-EE₂ may be
 351 more difficult to degrade. Our study corroborates their obser-
 352 vations, because the degradation of Sulfo-EE₂ is not elucidated
 353 well by known degradation rules or by FED-based theory.
 354

We now examine estrogenic potential using the number of
 355 hydrogen bond donating and accepting groups and the log P.
 356 Figure 3S shows these values for EE₂ and the initial metabolites.
 357 EHMD has lower estrogenic potential than EE₂ because the n_a
 358 is greater (3 vs 2), the n_d is unchanged, and the log P is smaller
 359 than that of EE₂ (2 vs 3.7). Sulfo-EE₂ also appears to have
 360 lower estrogenic potential than EE₂ for similar reasons. OH-EE₂
 361 has a lower log P (3.4 vs 3.7) and higher n_a (3 vs 2) compared
 362 to EE₂, but it also has an additional hydrogen bond donating
 363 group, a fact that may counterbalance the changes in log P and
 364 n_a. Thus, in this case the relative estrogenic potential is not as
 365 clear; however, we hypothesize that OH-EE₂ has less estrogenicity
 366 than EE₂ because previous work has shown that 2OH-E₂
 367 (not 2OH-EE₂) is less estrogenic than E₂.⁴⁵ If hydroxylation
 368 at C2 reduces estrogenicity for E₂, it seems reasonable to expect
 369 the same for EE₂.
 370

Estrogenic potential changes during the course of the trans-
 371 formation pathways. For example, during the EE₂-to-EDMC
 372 pathway (Figure 4S), there are clear indications that estrogenic
 373

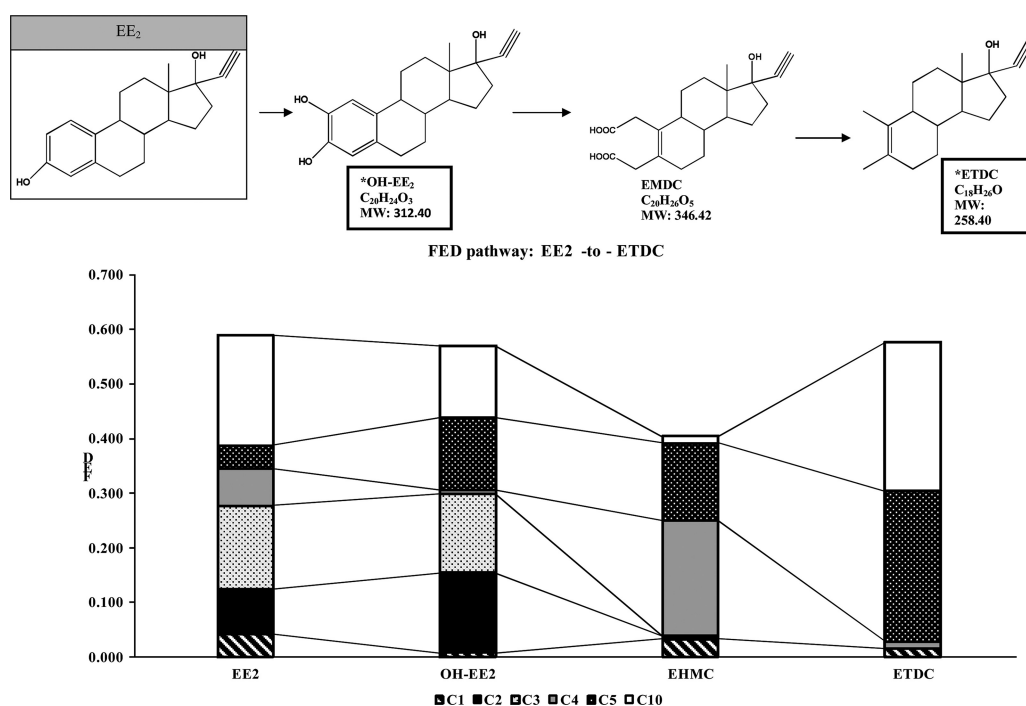


Figure 2. Predicted pathway for the degradation of EE₂ to ETDC. Measured metabolites are indicated with a bold highlight, and metabolites identified as part of this study are marked by an asterisk. Note the dramatic increase at carbon 4 as ring cleavage occurs (2OH to EHMC).

374 potential decreases during the steps leading to ring cleavage; 375 the log P decreases and the n_a increases. The last compound in 376 the pathway (EDMC) is without the active phenolic ring and 377 is therefore likely to have lower estrogenic potential. There are 378 however, two predicted metabolites (i.e., ETMD and CEDM) 379 that have a higher n_d (3 and 4 respectively) than EE₂. These 380 two compounds should probably be tested for estrogenicity 381 in future efforts. During the EE₂-ETDC pathway, there are also 382 indications that estrogenic potential is reduced (Figure 5S). 383 OH-EE₂ (as mentioned earlier) is likely less estrogenic than 384 EE₂, and EDMC has less estrogenic potential than OH-EE₂ 385 (or EE₂) because it has lower log P and higher n_a . The last com- 386 pound in this pathway (ETDC) has lost the active ring and 387 likely has lower estrogenic potential than EE₂. Finally, we hypo- 388 thesize that Sulfo-EE₂ has less estrogenic potential than EE₂ 389 because Sulfo-EE₂ has a lower log P than EE₂ (i.e., $3.0 < 3.7$, 390 Figure 6S) and Sulfo-EE₂ has a higher n_a ($5 > 2$, Figure 6S).^{42,43} 391 Sulfate conjugation does not change n_d .

392 ■ DISCUSSION

393 **Theory.** These results show that FED-based calculations 394 can be useful for understanding the transformation of EE₂. It is 395 interesting to observe that UHF-based FED solutions provide 396 guidance with respect to where electrophilic initiating reactions 397 take place, despite the fact that it does not rigorously account 398 for electron–electron interactions. The reason is because UHF 399 provides a broad accounting for electron–electron interactions 400 using the central field approximation. This approach allows 401 electron–electron interactions to be accounted for in a way that 402 is independent of angular coordinates (i.e., the precise location 403 of an electron associated with a particular orbital). The HF 404 solutions to the atomic wave function contain an electron– 405 electron interaction “correction” imbedded into the result, which 406 leads to numerical trends that are largely in line with DFT.

UHF is accurate enough for those interested in the initiating 407 reactions associated with EE₂. 408

Table 1 included four biologically produced structures that 409 do not appear in the transformation pathways presented in this 410 manuscript. This may reflect a need to investigate alternative 411 degradation rules, or it may point to limitations associated with 412 FED-based predictions. For example, the structures of DNDPA 413 ($m/z = 379$) and O–DNDPA ($m/z = 375$) show hydroxyl 414 groups and a double bond at C4. It is possible that these struc- 415 tures could appear in a pathway similar to the 6AH-EE₂ path- 416 way shown in this paper. Specifically, if 6AH-EE₂ is oxygenated 417 at C4 (which has the second highest FED value), the result is 418 a chemical structure that is a precursor for the two DNDPA 419 structures. Table 1 also shows OPCA ($m/z = 385$) and OPO 420 ($m/z = 309$), which show chemical modifications at low FED 421 carbon units. Predicting these structures may require other 422 reactivity indices. 423

The current results show that FED values increased at C4, 424 which is adjacent to the carbon atoms being attacked on ring A. 425 This result seems counterintuitive, because oxidation reactions 426 remove an electron from the highest molecular orbital, and 427 would presumably decrease the amplitude of the square of the 428 HOMO and therefore the FED (according to traditional fron- 429 tier molecular orbital theory). However, it is possible to observe 430 a local increase in electron density in a compound that is 431 subject to oxidation. This is RIER, which asserts that, when an 432 electron is removed from the highest molecular orbital, nearby 433 orbitals may “relax” and reconfigure so that the FED of a parti- 434 cular carbon atom may increase. This idea had been compu- 435 tationally demonstrated previously,⁴⁸ but it gained its strongest 436 support from recent experiments by Melin et al., 2007,⁴⁴ who 437 oxidized dinuclear cobalt and simultaneously reduced the chlo- 438 ranilate linker connecting the cobalt complexes. What appeared 439 as a computational anomaly now had stronger experimental 440

support. The presence of orbital relaxation should encourage the use of higher levels of electronic theory when exploring full transformation pathways because electron–electron interactions need to be rigorously accounted for.

Application. Practical aspects of EE₂ metabolism have taken shape. The first is related to ring cleavage, which is a key metabolic event because it produces metabolites that are easier to biodegrade. When EE₂ is degraded, ring A is cleaved first. This is supported by the identities of most of the measured metabolites presented in the literature, and it is also supported by the FED analysis presented here. Haiyan et al., 2007 proposed that ring B is cleaved first, based on the identity of metabolites produced by *Sphingobacterium* sp. JCRS, but their results appear to be the exception, rather than the rule.¹⁵ A second practical issue is related to Sulfo-EE₂. This metabolite has been independently identified from mixed cultures in three different studies, including this current effort. Khunjar et al., 2011 recently found that Sulfo-EE₂ was not degraded by heterotrophic cultures that were otherwise active. Our results support the notion that Sulfo-EE₂ is fairly resistant to biodegradation because of the presence of the sulfate group in ring A.¹³ Further, sulfate conjugation appears to cause recalcitrance for estrone, estradiol, estriol, which are similar to EE₂ in structure.^{46,49} Sulfo-EE₂ may either be a “dead-end” metabolite, or it may be transformable after desulfurization, which may be a slow process.^{49,50} Wastewater treatment plants that are interested in EE₂ should look for Sulfo-EE₂ in secondary effluent.

The broader application of FED-based theory is another issue of practical significance. A new tool enabling the *a priori* prediction of organic metabolites would be a valuable resource for environmental professionals, and there are subtle indications that the FED-based approach can help explain other transformations of interest. Estrone, estradiol, and estriol are conjugated at the carbon units that have high FED values.^{49,51–53} Kurisu et al., 2010 proposed an estradiol degradation pathway that is consistent with FED-based theory,⁵⁴ and Yi et al.⁵⁵ used NMR to identify trimethoprim byproducts that are in agreement with FED-based modeling. It is now possible to duplicate the current effort for other compounds, but it is also clear that future research can extend and improve FED-based modeling. For example, other approaches may better address resonance stability, which can cause high FED carbon units to be unreactive.⁵⁶ We used Rule 5 to account for this, but alternative approaches may improve model performance. The major challenge for future efforts will concern the proper incorporation of kinetics. FED-based techniques must account for the interactions between nonspecific enzymes (e.g., oxygenases, dehydrogenases, sulfotransferases) and high FED carbon sites, so that binding characteristics can be determined and reaction rates can be computed. A kinetically based FED approach can also reveal the impact of steric effects and shed light on the reversibility of these reactions. This type of model prediction needs to be judged against experimental data that quantifies metabolite concentrations as a function of time, and, at present, this kind of information is in very short supply. Fortunately, there is incentive to fill this data gap, as a kinetically based FED model can tell us the relative yield of different metabolites and help us discover others that are highly estrogenic.

■ ASSOCIATED CONTENT

Supporting Information

More details on the generation of metabolic pathways and estrogenic potential calculations. This material is available free of charge via the Internet at <http://pubs.acs.org>.

■ AUTHOR INFORMATION

Corresponding Author

*Phone: (412) 624-9548. Fax: (412) 624-0135. E-mail: wharper@pitt.edu.

■ ACKNOWLEDGMENTS

This work is based upon work supported by the National Science Foundation (NSF Grant No. BES-0827412). Any opinions, findings, and conclusions or recommendations expressed in this material are those of the authors and do not necessarily reflect the views of NSF. The authors thank the National Consortium for Graduate Degrees for Minorities in Engineering and Science and the K. Leroy Irvis Fellowship program for financial support provided to W.J.B. The authors also thank the anonymous reviewers for their helpful mixture of insight, advice, and encouragement.

■ REFERENCES

- (1) Kolpin, D.; Furlong, E.; Meyer, M.; Thurman, E.; Zaugg, S.; Barber, L.; Buxton, H. Pharmaceuticals, hormones, and other organic wastewater contaminants in U.S. streams, 1999–2000: A national reconnaissance. *Environ. Sci. Technol.* **2002**, *36* (6), 1202–1211.
- (2) Kuch, H. M.; Ballschmiter, K. Determination of endocrine-disrupting phenolic compounds and estrogens in surface and drinking water by HRGC-(NCI)-MS in the pictogram per liter range. *Environ. Sci. Technol.* **2001**, *35* (15), 3201–3206.
- (3) Baronti, C.; Curini, R.; D’Ascenzo, G.; Corcia, A. D.; Gentili, A.; Samperi, R. Monitoring natural and synthetic estrogens at activated sludge sewage treatment plants and in a receiving river. *Environ. Sci. Technol.* **2000**, *34* (24), 5059–5066.
- (4) Parkkonen, J.; Larsson, D.; Adolfsson-Erici, M.; Pettersson, M.; Berg, A.; Olsson, P.; Förlin, L. Contraceptive pill residues in sewage effluent are estrogenic to fish. *Mar. Environ. Res.* **2000**, *50* (1–5), 198.
- (5) Purdom, C. E.; Hardiman, P. A.; Bye, V. J.; Eno, N. C.; Tyler, C. R.; Sumpter, J. P. Estrogenic effects of effluents from sewage treatment works. *Chem. Ecol.* **1994**, *8*, 275–285.
- (6) Pawlowski, S.; Aerle, R. V.; Tyler, C. R.; Braunbeck, T. Effects of 17 α -ethinylestradiol in a fathead minnow (*Pimephales promelas*) gonadal recrudescence assay. *Ecotox. Environ. Safe.* **2004**, *57*, 330–345.
- (7) Bursch, W.; Fuerhacker, M.; Gemeiner, M.; Grillitsch, B.; Jungbauer, A.; Kreuzinger, N.; Moestl, E.; Scharf, S.; Schmid, E.; Skutan, S.; Walter, I. Endocrine Disrupters in the aquatic environment: The Austrian approach- ARCEM. *Water Sci. Technol.* **2004**, *50*, 293–300.
- (8) Yi, T.; Harper, W. F. The link between nitrification and biotransformation of 17 α -ethinylestradiol. *Environ. Sci. Technol.* **2007**, *41* (12), 4311–4316.
- (9) Shi, J.; Fujisawa, S.; Nakai, S.; Hosomi, M. Biodegradation of natural and synthetic estrogen by nitrifying activated sludge and ammonia-oxidizing bacterium *Nitrosomonas europaea*. *Water Res.* **2004**, *38* (9), 2323–2330.
- (10) Dytczak, M. A.; Londry, K. L.; Oleszkiewicz, J. A. Transformation of estrogens in nitrifying sludge under aerobic and alternating anoxic/aerobic conditions. 79th Annual Water Environment Federation Technical Exposition and Conference, Dallas, TX, October 2006.
- (11) Gaulke, L. S.; Strand, S. E.; Kalhorn, T. F.; Stensel, H. D. 17 α -ethinylestradiol transformation via abiotic nitration in the presence of ammonia-oxidizing bacteria. *Environ. Sci. Technol.* **2008**, *42* (20), 7622–7627.

- (12) Gussemé, B. D.; Pycke, B.; Hennebel, T.; Marcoen, A.; Vlaeminck, S. E.; Noppe, H.; Boon, N.; Verstraete, W. Biological removal of 17 α -ethinylestradiol by a nitrifier enrichment culture in a membrane bioreactor. *Water Res.* **2009**, *43*, 2493–2503.
- (13) Khunjar, W. O.; Mackintosh, S.; Skotnicka-Pitak, J.; Baik, S.; Aga, D. S.; Love, N. G. Elucidating the role of ammonia-oxidizing bacteria versus heterotrophic bacteria during the biotransformation of 17 α -ethinylestradiol and trimethoprim. *Environ. Sci. Technol.* **2011**, *45* (8), 3605–3612.
- (14) Yi, T.; Mackintosh, S.; Aga, D. S.; Harper, W. F. Exploring 17 α -ethinylestradiol removal, mineralization and bioincorporation in engineered bioreactors. *Water Res.* **2011**, *45* (3), 1369–1377.
- (15) Lehninger, A.; Nelson, D.; Cox, M. *Principles of Biochemistry*, 2nd ed.; Worth Publishers: New York, NY, 1999.
- (16) Fang, H.; Tong, W.; Shi, L. M.; Blair, R.; Perkins, R.; Branham, W.; Hass, B. S.; Xie, Q.; Dial, S. L.; Moland, C. L.; Sheehan, D. M. Structure-activity relationships for a large diverse set of natural, synthetic, and environmental estrogens. *Chem. Res. Toxicol.* **2001**, *14*, 280–294.
- (17) Haiyan, R.; Shulan, J.; Naeemud din Ahmad.; Dao, W.; Chengwu, C. Degradation characteristics and metabolic pathway of 17 α -ethinylestradiol by *Sphingobacterium* sp. JCR5. *Chemosphere* **2007**, *66* (2), 340–346.
- (18) Lipinski, C. A.; Lombardo, F.; Dominy, B. W.; Feeney, P. J. Experimental and computational approaches to estimate solubility and permeability in drug discovery and development settings. *Adv. Drug Delivery Rev.* **2001**, *46*, 3–26.
- (19) Schultz, T. W.; Sinks, G. D.; Cronin, M. T. D. Structure-activity relationships for gene activation oestrogenicity: Evaluation of a diverse set of aromatic chemicals. *Environ. Toxicol.* **2002**, *17*, 14–23.
- (20) Fukui, K.; Yonezawa, T.; Shingu, H. A molecular orbital theory of reactivity in aromatic hydrocarbons. *J. Chem. Phys.* **1952**, *20* (4), 722–725.
- (21) Wheland, G.; Pauling, L. A quantum mechanical discussion of orientation of substituents in aromatic molecules. *J. Am. Chem. Soc.* **1935**, *57*, 2086–2095.
- (22) Ohko, Y.; Iuchi, K. I.; Niwa, C.; Tatsuma, T.; Nakashima, T.; Iguchi, T.; Kubota, Y.; Fujishima, A. 17 β -estradiol degradation by TiO₂ photocatalysis as a means of reducing estrogenic activity. *Environ. Sci. Technol.* **2002**, *36* (19), 4175–4181.
- (23) Ohura, T.; Amagai, T.; Sugiyama, T.; Fusaya, M.; Matsushita, H. Occurrence, profiles, and photostabilities of chlorinated polycyclic aromatic hydrocarbons associated with particulates in urban air. *Environ. Sci. Technol.* **2005**, *39* (1), 2045–2054.
- (24) Lee, B. D.; Iso, M.; Hosomi, M. Prediction of Fenton oxidation positions in polycyclic aromatic hydrocarbons by Frontier electron density. *Chemosphere* **2001**, *42*, 431–435.
- (25) Endocrine disruption [electronic resource]: biological basis for health effects in wildlife and humans; Norris, D. O., Carr, J. A. Oxford University Press: New York, 2006; xiv, 477 p.; ill.; 25 cm.
- (26) Skotnicka-Pitak, J.; Khunjar, W. O.; Aga, D. S.; Love, N. G. Characterization of metabolites formed during the biotransformation of 17 α -ethinylestradiol by *Nitrosomonas europaea* in batch and continuous flow bioreactors. *Environ. Sci. Technol.* **2009**, *43* (10), 3549–3555.
- (27) Frisch, M. J.; Trucks, et al. Revision C.02 ed.; Gaussian, Inc.: Wallingford, CT, 2004.
- (28) Becke, A. D. Density-functional thermochemistry. III. The role of exact exchange. *J. Chem. Phys.* **1993**, *98*, 5648–5652.
- (29) Lee, C.; Yang, W.; Parr, R. G. Development of the Colle-Salvetti correlation-energy formula into a functional of the electron density. *Phys. Rev.* **1988**, *37*, 785–789.
- (30) Kamath, A. V.; Vaidyanathan, C. S. New pathway for the biodegradation of indole by *Aspergillus niger*. *Appl. Environ. Microbiol.* **1990**, *56*, 275.
- (31) Hay, A. G.; Focht, D. D. Cometabolism of 1,1-dichloro-2,2-bis(4-chlorophenyl)ethylene by *Pseudomonas acidovorans* M3GY grown on biphenyl. *Appl. Environ. Microbiol.* **1998**, *64*, 2141.
- (32) Nosova, T.; Jousimies-Summer, H.; Kaihovaara, P.; Jokelainen, K.; Heine, R.; Salaspuro, M. Characteristics of alcohol dehydrogenases of certain aerobic bacteria representing human colonic flora. *Alcohol. Clin. Exp. Res.* **1997**, *21*, 489.
- (33) Nagy, P. I.; Fabian, W. M. F. Theoretical study of the enol-imine – enamionetautomeric equilibrium in organic solvents. *J. Phys. Chem. B* **2006**, *110*, 25026–25032.
- (34) Steffan, R. J.; McClay, K.; Vainberg, S.; Condee, C. W.; Zhang, D. Biodegradation of the gasoline oxygenates methyl tert-butyl ether, ethyl tert-butyl ether, and tert-amyl methyl ether by propane-oxidizing bacteria. *Appl. Environ. Microbiol.* **1997**, *61*, 4216.
- (35) Casellas, M.; Grifoll, M.; Bayona, J. M.; Solanas, A. M. New metabolites in the degradation of fluorine by *Arthrobacter* sp. Strain F101. *Appl. Environ. Microbiol.* **1997**, *63*, 819.
- (36) Dean-Ross, D.; Moody, J. D.; Freeman, J. P.; Doerge, D. R.; Cerniglia, C. E. Metabolism of anthracene by a *Rhodococcus* species. *FEMS Microbiol. Lett.* **2001**, *204*, 205.
- (37) Brzostowicz, P. C.; Walters, D. M.; Jackson, R. E.; Halsey, K. H.; Ni, H.; Rouviere, P. E. Proposed involvement of soluble methane monoxygenase homologue in the cyclohexane dependent growth of a new *Brachymonas* species. *Environ. Microbiol.* **2005**, *7*, 179.
- (38) Nakazawa, T.; Hayashi, E. Phthalate and 4-hydroxyphthalate metabolism in *Pseudomonas testosterone*: Purification and properties of 4,5 dihydroxyphthalate decarboxylase. *Appl. Environ. Microbiol.* **1978**, *36*, 264.
- (39) Olsen, R. H.; Kukor, J. J.; Kaphammer, B. A novel toluene-3-monoxygenase pathway cloned from *Pseudomonas pickettii* PK01. *J. Bacteriol.* **1994**, *176*, 3749.
- (40) Viswanadhan, V. N.; Ghose, A. K.; Revankar, G. R.; Robins, K. R. Atomic physicochemical parameters for three dimensional structure directed Quantitative Structure-Activity Relationships 4. Additional Parameters for hydrophobicity and dispersive interactions and their application for an automated superposition of certain naturally occurring nucleoside antibiotics. *J. Chem. Inf. Comput. Sci.* **1989**, *29*, 163–172.
- (41) Madigan, M. T., Martinko, J. M. Parker, J. *Brock biology of microorganisms*; Prentice-Hall: Upper Saddle River, NJ, 1997.
- (42) Della Greca, M.; Pinto, B.; Pistillo, P.; Pollio, A.; Previtiera, L.; Temussi, F. Biotransformation of ethinylestradiol by microalgae. *Chemosphere* **2008**, *70*, 2047–2053.
- (43) Lengeler, J. W., Drews, G., Schlegel, H. *Biology of the Prokaryotes*; Georg ThiemeVerlag: Rudigerstrasse 14, D. Stuttgart, Germany, 1999.
- (44) Melin, J.; Ayers, P.; Ortiz, J. Removing electrons can increase electron density: A computational study of negative Fukui functions. *J. Phys. Chem. A* **2007**, *111*, 10017–10019.
- (45) Lee, Y.; Escher, B. I.; von Gunten, U. Efficient removal of estrogenic activity during oxidative treatment of waters containing steroid estrogens. *Environ. Sci. Technol.* **2008**, *42* (17), 6333–6339.
- (46) Kotov, A.; Falany, L.; Wang, J.; Falany, C. Regulation of estrogen activity by sulfation in human Ishikawa endometrial adenocarcinoma cells. *J. Steroid Biochem. Mol. Biol.* **1999**, *68*, 137–144.
- (47) Zamek-Gliszczynski, M. J.; Hoffmaster, K. A.; Nezasa, K. I.; Tallman, M. N.; Brouwer, K. L. R. Integration of hepatic drug transporters and phase II metabolizing enzymes: Mechanisms of hepatic excretion of sulfate glucuronide, and glutathione metabolites. *Eur. J. Pharm. Sci.* **2006**, *27*, 447–486.
- (48) Bartolotti, L. J.; Ayers, P. W. An example where orbital relaxation is an important contribution to the Fukui function. *J. Phys. Chem. A* **2005**, *109*, 1146–1151.
- (49) Hutchins, S. R.; White, M. V.; Hudson, F. M.; Fine, D. D. Analysis of lagoon samples from different concentrated animal feeding operations for estrogens and estrogen conjugates. *Environ. Sci. Technol.* **2007**, *41* (3), 738–744.
- (50) D’Ascenzo, G. D.; DiCorcia, A.; Gentili, A.; Mancini, R.; Mastropasqua, R.; Nazzari, M.; Samperi, R. Fate of natural estrogen conjugates in municipal sewage transport and treatment facilities. *Sci. Total Environ.* **2003**, *302*, 199–209.

- 697 (51) Komori, K.; Tanaka, H.; Okayasu, Y.; Yasojima, M.; Sato, C.
698 Analysis and occurrence of estrogen in wastewater in Japan. *Water Sci.*
699 *Technol.* **2004**, *50* (5), 93–100.
- 700 (52) Liu, Z.; Kanjo, Y.; Mizutani, S. Simultaneous analysis of natural
701 free estrogens and their sulfate conjugates in wastewater. *CLEAN*
702 **2010**, *38* (12), 1146–1151.
- 703 (53) Koh, Y.; Chiu, T.; Boobis, A. R.; Scrimshaw, M. D.; Bagnall,
704 J. P.; Soares, A.; Pollard, S.; Cartmell, E.; Lester, J. N. Influence of
705 operating parameters on the biodegradation of steroid estrogens and
706 nonylphenolic compounds during biological wastewater treatment
707 processes. *Environ. Sci. Technol.* **2009**, *43* (17), 6646–6654.
- 708 (54) Kurisu, F.; Ogura, M.; Saitoh, S.; Yagi, O. Degradation of natural
709 estrogen and identification of the metabolites produced by soil isolates
710 of *Rhodococcus* sp. and *Sphingomonas* sp. *J. Biosci. Bioeng.* **2010**,
711 *109* (6), 576–582.
- 712 (55) Yi, T.; Barr, W.; Harper, W. F. Electron density-based
713 transformation of trimethoprim during biological wastewater treat-
714 ment. *Water Sci. Technol.* In press.
- 715 (56) Jaramillo, C.; Guerra, D.; Moreno, L. F.; Restrepo, A. Com-
716 petitive substituent effects on the reactivity of aromatic rings. *J. Phys.*
717 *Chem A* **2010**, *114* (19), 6033–6038.